

## Processing the PK324 Duplex Stainless Steel: Influences on hot deformability of the as-cast microstructure

### Izdelava dupleksnega nerjavnega jekla PK324: Vplivi na vročo preoblikovalnost lite mikrostrukture

TATJANA VEČKO PIRTOVŠEK<sup>1</sup>, PETER FAJFAR<sup>1</sup>,\*

<sup>1</sup>University of Ljubljana, Faculty of Natural Science and Engineering, Department of Materials and Metallurgy, Aškerčeva 12, SI-1000 Ljubljana, Slovenia

\*Corresponding author. E-mail: peter.fajfar@ntf.uni-lj.si

**Received:** April 8, 2009

**Accepted:** May 27, 2009

**Abstract:** Examination of reasons that cause cracking of the as-cast microstructure of the PK324 duplex stainless steel (DSS) during the hot working process represents an important step to improve the final quality of product. Hot compression tests were applied in the examination and they were combined with the observations in light microscope. Deformation behaviour of initial as-cast samples as well of the samples after ten hours ageing has been studied with the Gleeble 1500D thermo-mechanical simulator. Applied strain rate was in the range of  $0.1 \text{ s}^{-1}$  to  $5 \text{ s}^{-1}$ , temperature interval was 900–1300 °C and strains were up to 0.7. Ten hours aged samples exhibited considerably narrower temperature range (interval) of safe hot deformation. Calculated activation energy for the entire range of the hot working process and for peak stresses was 287 kJ/mol.

**Izveček:** Za izboljšanje kvalitete končnih izdelkov iz dupleksnega nerjavnega jekla PK324 (DSS) so pomembne preiskave vzrokov za nastanek razpok med vročim preoblikovanjem. Za preiskovalni metodi smo uporabili vroče tlačne preizkuse in optično mikroskopijo. Preizkuse za določevanje preoblikovalnih lastnosti dupleksnega jekla v litem stanju ter v stanju po deseturnem homogenizacijskem žarjenju smo izvajali na simulatorju termomehanskih stanj Gleeble 1500D. Preizkusi so bili izvedeni v območju hitrosti deformacije od  $0,1 \text{ s}^{-1}$  do  $5 \text{ s}^{-1}$ , v temperaturnem intervalu 900–1300 °C ter pri

stopnji deformacije do 0,7. Temperaturno področje, ki zagotavlja deformacijo brez nastanka razpok, je za žarjene vzorce bistveno ožje kot za lite. Izračunana navidezna aktivacijska energija za vroče preoblikovanje pri največjih napetostih in na celotnem temperaturnem področju je 287 kJ/mol.

**Key words:** PK324 duplex stainless steel, as-cast microstructure, aging treatment, hot compression

**Ključne besede:** dupleksno nerjavno jeklo PK324, lita mikrostruktura, žarjena mikrostruktura, vroče stiskanje

## INTRODUCTION

Duplex stainless steels (DSS) are constantly gaining their importance due to good combination of their corrosion resistance and of mechanical and physical properties in a wide temperature interval when compared to standard austenitic stainless steels, and they have found their applications in chemical and paper industry, in shipbuilding, as welding materials, in petroleum industry, etc. The obtained properties of super duplex stainless steel result in balanced alloying with the ferrite - (Cr, Mo, Si, etc.) and austenite-forming elements (Ni, Mn, C, N, etc.). Thus steel consists of a two-phase matrix, i.e. of austenite and ferrite, where austenite ( $\gamma$ ) contributes toughness while ferrite ( $\alpha$ ) improves the mechanical and welding characteristics. Their properties have been continually improved by optimization of alloying, hot and cold working, heat treatment, etc.<sup>[1-6]</sup>.

It is well known that hot working of dual-phase steel is a very demanding one since possible problems are usually more intricate in comparison to working single-phase steel especially when the as-cast material is taken in account. Interface boundary sliding (IBS) seems to be the major deformation mechanism in the duplex steel at higher strain rates ( $> 1 \text{ s}^{-1}$ ) and relatively low temperatures (about 1000 °C). Precipitation of intermetallic phases (sigma ( $\sigma$ ),  $\text{Cr}_2\text{N}$ , Chi phases ( $\chi$ ), etc) in the approximate temperature interval of 500–1050 °C additionally reduces the range of safe hot working therefore the process has to be performed at temperatures above the interval of precipitation of intermetallic phases. Hot working of the as-cast material represents critical step in the production cycle since the as-cast microstructure is very prone to cracking, especially on the ferrite/austenite ( $\alpha/\gamma$ ) grain boundaries (it has been observed also on the  $\alpha/\alpha$  and  $\gamma/\gamma$  grain

boundaries) since there eventually impurities and carbides precipitate (usually  $M_7C_3$  and  $M_{23}C_6$ ). Furthermore, both phases have different crystallographic structures and deformation modes, different strengths (austenite is significantly stronger in the range of hot working) and softening mechanisms (and rates too). On the other hand, DSS can exhibit excellent hot plasticity if the microstructure is fine enough<sup>[6–16]</sup>.

The PK324 DSS is usually used as welding material and it belongs to the group of duplex stainless steel, and cracking during the hot working process, especially when cast ingots are worked, is still its disadvantage. This paper represents a contribution to elucidation of reasons for appearance of cracking of the as-cast microstructure in hot working the PK324 DSS.

#### APPLIED METHODS FOR CHARACTERIZATION, TESTING AND MATERIALS

An ingot of PK324 DSS weighing 380 kg has been cast in a vacuum electric furnace. Chemical composition of the applied batch is given in Table 1; from the Table is thus visible that the batch contained mass fraction 0.10 % of C, 30.1 % of Cr and 9.5 % of Ni. Test specimens (cylindrical specimens with dimensions  $\phi = 10 \text{ mm} \times 15 \text{ mm}$ ) were

taken from the ingot cross sections and half of them was additionally aged at 1250 °C for 10 h. Both groups of samples were hot compressed (Figure 1a) in the Gleeble 1500D thermo-mechanical simulator at three strain rates ( $0.1 \text{ s}^{-1}$ ,  $1 \text{ s}^{-1}$  and  $5 \text{ s}^{-1}$ ), in the temperature interval of 950–1300 °C and with strains up to 0.7. Cylindrical specimens were heated to the deformation temperature in 5 min. A 5 min holding time, hot compression and gas cooling followed (Figure 1b). (LM) ZEISS JENA VERT microscope was applied in the light microscopy, and Murakami etchant<sup>[17]</sup> was used in order to colour  $\sigma$  phase grey,  $\alpha$  phase brown, carbides red, green and blue, while  $\gamma$  phase remained uncoloured. XRD (X-ray diffraction, Cristallogflex 4 apparatus) was used to determine fractions of phases in the microstructures. All the experiments and testing conditions as well as the applied characterizations in the examinations are presented in Table 2.

The initial as-cast microstructure is presented in Figure 2; the microstructure consisted of  $\gamma$  phase in the interdendritic spaces and of  $\alpha$  phase. Amount of ferrite of about 48 %, of austenite of about 52 % were found in the samples taken from the ingot centre, while the amount of sigma phase was below 1 %, and amount of carbides ( $M_{23}C_6$  and  $M_7C_3$ ) at about 0.3 %, measured at the room temperature. Carbides predomi-



## RESULTS AND DISCUSSION

The obtained flow stress curves with the as-cast samples taken from the ingot head and for  $0.1 \text{ s}^{-1}$  strain rate are presented in Figure 3; steady-state flow was achieved with the initial as-cast material. At higher deformation temperatures, i.e. above  $1150 \text{ }^{\circ}\text{C}$ , where the fraction of ferrite was considerably higher<sup>[16]</sup>, the flow curves after achieving maximal values retained those levels since dynamic recovery of ferrite occurred during the hot deformation. Ferrite has namely high stacking-fault energy that favours dynamic recovery (DRV). On the other hand, at deformation temperatures below  $1150 \text{ }^{\circ}\text{C}$  the fraction of austenite was higher in comparison to the upper temperature interval ( $1150\text{--}1250 \text{ }^{\circ}\text{C}$ ); dynamic recrystallization (DRX) led to reduced values of flow stresses after achieving the peak values. The phenomenon of DRX of austenite was indicated also by shifts of peak values of flow curves to higher strains at decreased deformation temperatures. The shape of flow curves at  $1 \text{ s}^{-1}$  strain rate was similar to that of curves for  $0.1 \text{ s}^{-1}$  strain rate while the peaks at the strain rate  $5 \text{ s}^{-1}$  were not so pronounced since they were more elongated like in hot compression of DSS at higher strain rates<sup>[13]</sup>.

The results about appearance or not appearance of cracks on free surfaces of compressed not aged and 10 h aged

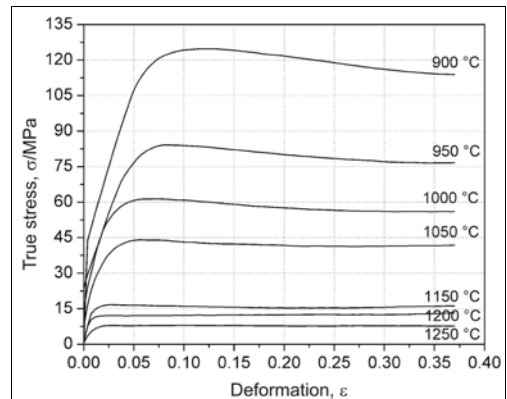


**Figure 3.** Flow stress curves of the as-cast PK324 DSS at various compression temperatures and at  $0.1 \text{ s}^{-1}$  strain rate

samples (see Figure 4a–b) are presented in Table 3 for the entire examined temperature interval. The results from the table indicated that good hot deformability was achieved with the non-aged as-cast samples in the temperature range  $1150\text{--}1250 \text{ }^{\circ}\text{C}$  while cracks were observed on deformed specimens bellow mentioned range. This could be attributed to the increased fraction of austenite<sup>[16]</sup> at temperatures below  $1150 \text{ }^{\circ}\text{C}$ , to different deformation modes as well as to different strengths of austenite and ferrite, etc. that led to crack formation on the  $\alpha/\gamma$  grain boundaries.

The obtained microstructures of compressed samples at various deformation temperatures are given in Figure 5. The microstructure became finer with the decreased compression temperature since the content of austenite increased; DRX namely took place in

austenite. Formation of austenite on the  $\alpha/\gamma$  and  $\alpha/\alpha$  grain boundaries which were sub-boundaries or boundaries of grains began during the hot deformation and the followed cooling. Microstructure of samples being deformed in the 1200–1250 °C temperature range consisted of ferrite and austenite that were in equilibrium at the deformation temperature, of Widmanstätten austenite that was formed during the cooling after the deformation, and of a small amount of carbides on the  $\alpha/\gamma$  grain boundaries (Figure 5a). Equilibrium between ferrite and austenite was achieved at those temperatures almost after ten minutes<sup>[16]</sup>. Further, dynamic softening process in the mentioned temperature range was very intensive since number of initial spots potentially suitable for precipitation of austenite during the cooling process after the hot deformation was reduced; consequently, austenite precipitated predominately on the  $\alpha/\gamma$  grain boundaries. The obtained microstructures of samples being deformed at lower temperatures (below 1150 °C) (Figure 5b-d) differed from the microstructures of samples that were deformed at temperatures above the mentioned ones. At latter temperatures the softening process was considerably less pronounced, thus many spots potentially suitable for nucleation and consequently also for precipitation of austenite ( $\alpha \rightarrow \gamma$ ) during the cooling process were available.

On the other hand, 10 h aged samples exhibited considerably narrower temperature range of safe hot deformation, i.e. 1200–1250 °C, in comparison to the non-aged samples (1150–1250 °C (Table 3)). This could be attributed to different  $\alpha \rightarrow \gamma$  transformation kinetics of the not aged and of the 10 h aged samples during the hot deformation. Microstructures of deformed and 10 h aged samples are given in Figure 6a and 6b for the deformation temperatures of 1250 °C and 1150 °C, respectively. Comparison of Figure 5a–b and Figure 6a–b revealed that approximately equal fractions of austenite and ferrite were found in both cases, but the grains in the 10 h aged samples were coarser. On the other hand, approximately 10–25 % higher values of steady-state flow stresses were obtained with the 10 h aged samples in comparison to the not aged samples. This could indicate that higher amount of ferrite was transformed into austenite during the hot deformation and this could be explained in the following way: a higher fraction of ferrite existed in the microstructure of samples being aged for 10 h before the hot deformation, thus higher non-equilibrium ferrite/austenite ratio existed at lower deformation temperatures. Consequently higher transformation (precipitation) rate of austenite took place in the entire ferrite phase and not only on the grain boundaries. Furthermore, the fraction of transformed austenite

was not higher in comparison to that in the not aged samples since there was not enough time for transformation, but austenite probably precipitated in a different way and the difference of its distribution could be observed. Thus the temperature range of safe hot working was narrower with the 10 h aged samples. The results on microanalyses on 10 h aged samples at 1250 °C (before hot compression) indicate that differences in contents of Cr and Ni between  $\alpha$  and  $\gamma$  phase seems to decrease, i.e. trying to reach the equilibrium between

both phases. Thus the content of Cr decreases and of Ni increases in  $\alpha$  while the opposite behaviour for both chemical elements in  $\gamma$  was found (these results will be published in next article). The state of material similar to that obtained after 10 h aging could be obtained also at slow solidification rates of DSS (segregations) that could result in reduced range of safe hot working of as-cast microstructure. For more accurate explanation of these results further examinations should be done.

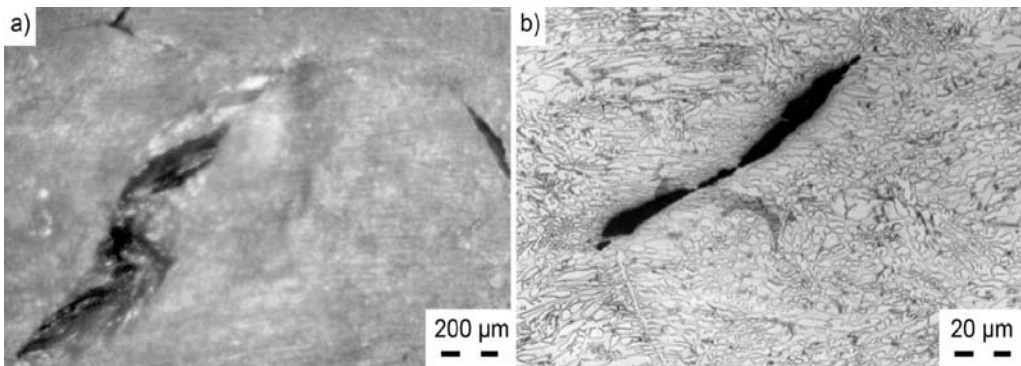


**Figure 4.** Appearance of cracking phenomenon on compressed samples; macro view (a), and micro view (cracking on grain boundaries) (b)

**Table 3.** Appearance of surface cracks as a function of compression temperature for as-cast state, not aged, and 10 h aged samples, strain rate  $1 \text{ s}^{-1}$ .

Deform. temp. $T/^\circ\text{C}$		900	950	1000	1050	1100	1150	1200	1250	1300
Cracking	Non-aged	Y	Y	S	S	S	N	N	N	Y
	10 h aged	Y	Y	Y	Y	Y	S	N	N	Y

N - without cracks, Y - deep cracks, S - fine cracks.

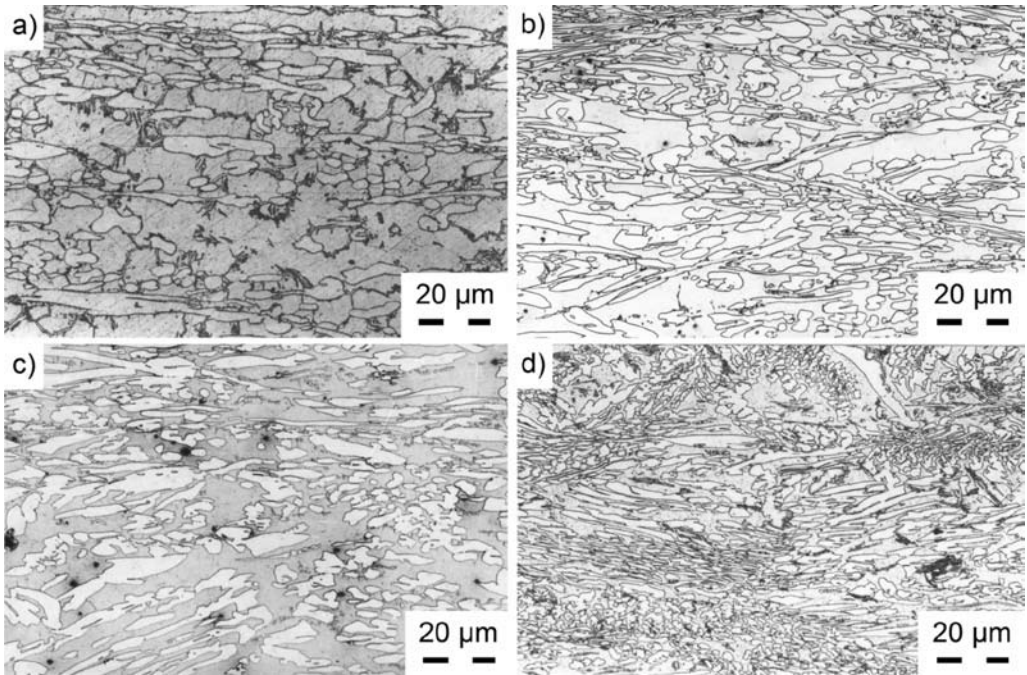


**Figure 5.** Obtained microstructures at  $1 \text{ s}^{-1}$  strain rate and at various compression temperatures: 1250 °C (a), 1150 °C (b), 1100 °C (c), and 950 °C (d), non-aged samples, gas cooling

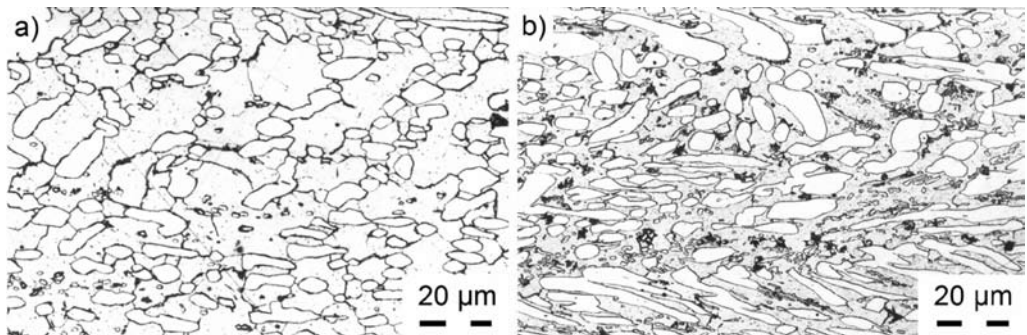


**Figure 6.** Obtained microstructures at  $1 \text{ s}^{-1}$  strain rate and at various compression temperatures: 1200 °C (a), 1150 °C (b), samples 10 h aged at 1250 °C, gas cooling

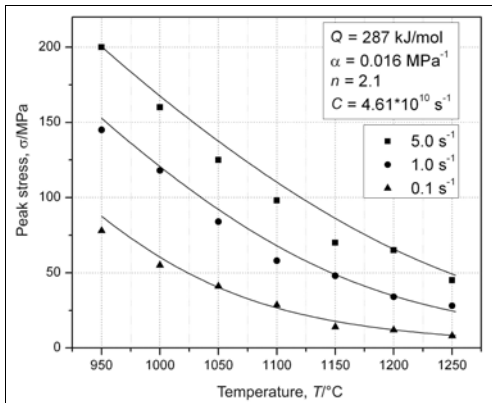


**Figure 7.** Comparison between the calculated and the measured peak stresses as a function of temperature, not aged, as-cast.

In order to determine activation energies by the procedure given in reference<sup>[18]</sup>, the values of peak stresses for the initial as-cast samples were fitted to the empirical sine-hyperbolic equation:

$$\dot{\epsilon} = A[\sinh(\alpha\sigma)]^n \exp\left(-\frac{Q}{RT}\right) \quad (1)$$

$Q$  represented the deformation activation energy,  $R$  the universal gas constant, and  $n$ ,  $\alpha$  and  $A$  materials constants. Activation energy at temperatures of examinations and for the applied strain rate ranges was calculated to be 287 kJ/mol. The comparison between the calculated and the measured values of peak stresses together with the other parameters of the equation (1) is given in Figure 7. The obtained activation energy was somewhat lower than that cited by other authors, e.g. CABRERA et al<sup>[9]</sup> for 25Cr7Ni3.8Mo DSS

( $Q = 438$  kJ/mol), and PAUL et al<sup>[15]</sup> ( $Q = 360$  kJ/mol). This could be attributed to considerably higher fraction of ferrite in our steel.

## CONCLUSIONS

Hot deformation behaviour of the PK324 DSS samples, as-cast, and 10 h aged at 1250 °C, was examined at strain rates 0.1–5 s<sup>-1</sup> and in the 950–1300 °C temperature range. The following conclusions could be made:

- Compression temperature played important role in the deformability of the as-cast microstructure. Appearance of surface cracking in hot compression below 1150 °C and no cracking above that temperature was observed with the not aged samples. Cracking occurred predominately on the  $\alpha/\gamma$  grain boundaries.
- Ten hours aged samples at 1250 °C could be safely deformed only in the temperature range 1200–1250 °C.
- The as-cast microstructure could be broken in the temperature range of 1150–1250 °C, otherwise the work-piece should be reheated to above 1150 °C.
- Calculated activation energy for the hot deformation process and for the peak values of flow stresses was 287 kJ/mol, and it was lower in

comparison to the cited values by other authors since our DSS contained higher fraction of ferrite.

## REFERENCES

- [1] JOSEFSSON, B., NILSSON, J. O., WILSON, A. (1992): Phase transformation in duplex steels and relation between continuous cooling and isothermal heat treatment, in: Duplex stainless steels. Ed.: J. Charles and S. Bernhardsson, *Beaune Bourgogne*, France; pp. 28–30.
- [2] NILSON, J. O. (1992): Super duplex stainless steels. *Materials Science and Engineering*; Vol. 8, pp. 685–700.
- [3] MARTINS, M., RODRIGUES, L. (2008): Effect of aging on impact properties of ASTM A890 Grade 1C super duplex stainless steel. *Materials Characterization*; Nogueira Forti, Vol. 59/2, pp. 162–166.
- [4] Charles, J., Bernhardsson, S. (1991): Duplex Stainless Steel. *Les editions de physique les Ulis*; France, pp. 3–48.
- [5] F. H. Hayes, M. G. Herherington, R. D. Longbottom, Thermodynamics of duplex stainless steels, *Materials Science and Engineering*, 6 (1990) 263–272.
- [6] C. H. Shek, K. W. Wong, J. K. L. Lai and D. J. Li, Hot tensile properties of 25Cr-8Ni duplex stainless steel containing cellular ( $\sigma+\gamma_2$ ) structure after various thermal treatments, *Materials Science and Engineering A*, 231/(1-2) (1997) 42–47.
- [7] MARTINS, M., CARLOS CASTELETTI, L. (2005): Heat treatment temperature influence on ASTM A890 GR 6A super duplex stainless steel microstructure. *Materials Characterization*; Vol. 55/3, pp. 225–233.
- [8] CHI-SHANG HUANG, CHIA-CHANG SHIH (2005): Effects of nitrogen and high temperature aging on  $\sigma$  phase precipitation of duplex stainless steel. *Materials Science and Engineering*; Vol. 402/(1–2), pp. 66–75.
- [9] CABRERA, J. M., MATEO, A., LLANES, L., PRADO, J. M., ANGLADA, M. (2003): Hot deformation of duplex stainless steels. *Journal of Materials Processing Technology*; pp.143–144, pp. 321–325.
- [10] YASUHIRO MAEHARA (1992): Effect of microstructure on hot deformation in duplex stainless steels. *Scripta Metallurgica et Materialia*; Vol. 26/11, pp. 1701–1706.
- [11] MOMENI, A., ABBASI, S. M., SHOKUH-FAR, A. (2007): Hot compression behaviour of as-cast precipitation-hardening stainless steel. *Journal of Iron and Steel Research International*; Vol. 14/5, pp. 66–70.
- [12] DUPREZ, L., COOMAN, B. C., AKDUT, N. (2002): Flow Stress and Ductility of Duplex Stainless Steel during High Temperature Torsion Deformation. *Metallurgical and Materials Transactions*; 33A, pp. 1931–1938.
- [13] ARBOLEDAS, J. M., MARTOS TIRADO, J. L., SANCHEZ RODRIGUES, R. (1996): Optimizing the hot deformability of 2205 duplex stainless steel by thermal/mechanical simulation, Proceedings of Stainless steels. *German Iron and Steel Institute*.

- [14] HAN, Y. S., HONG, SOON H. (1999): Microstructural changes during superplastic deformation of Fe-24Cr-7Ni-3-Mo-0.14N duplex stainless steel. *Materials Science and Engineering*; Vol. 266, pp. 276–284.
- [15] PAUL, A., MARTOS, J. L., SANCHEZ, R. (1993): Behaviour of 2205 Duplex stainless steel under hot working conditions. *Innovation Stainless steel*; Florence, Italy, 11–14, pp. 3297–3302.
- [16] FAZARINC, M., VEČKO PIRTOVŠEK, T., BOMBAČ, D., KUGLER, G., TERČELJ, M. (2008): Processing of PK 324 duplex stainless steel: influence of aging temperature and cooling rates on precipitation: preliminary results. *RMZ*; Vol. 55, pp. 420–431.
- [17] KLEMM, B. (1962): *Handbuch der metallographischen Ätzverfahren*. Deutsche Verlag für Grundstoffindustrie, Leipzig.
- [18] KUGLER, G., KNAP, M., PALKOWSKI, H., TURK, R. (2004): Estimation of activation energy for calculating the hot workability properties of metals. *Metallurgija*; Vol. 43, pp. 267–272.